structure described by the CIF can then be imported into to the user's graphics or Rietveld package.

Free-text searches of the comments are also included on this screen. These are particularly useful, as ICSD collection codes and CSD refcodes are included in the comments. If the user has the CSD installed on the same machine as the PDF, the PDF entry links live to the coordinates in the CSD entry.

By using the Results menu option when a hit list is displayed, ranges of cells in the spreadsheet can be selected and simple descriptive statistics (mean, median and estimated standard deviation) can be generated. Also under Results is a Graph Fields option. The variables used for the *x* and *y* axes of the plot can be selected and both scatter plots and histograms can be generated. Each of the points in such a plot is 'live' and can be clicked to display the full PDF entry. Fig. 3.7.1 shows a plot of the cubic lattice parameter with respect to at.% Fe in FeO (Fe and O only, space group No. 225) under ambient conditions. From such data it is easy to generate a correlation between the Fe stoichiometry and the lattice parameter.

An optional add-on module to the PDF is *SIeve* (Search Index). This is a peak-based search/match program which enables the use of a manually entered (or imported) peak list or derives a peak list from imported ASCII raw powder-diffraction data in several formats. It also has a flexible ASCII data-import module. Hanawalt, Fink, Long8 (the eight lowest-angle peaks in the pattern) or electron-diffraction searches can be carried out. Again, there is a Preferences option to customize the searches. A particularly useful (and easy-to-use) feature is the ability to apply a filter to the search/match. This filter can be selected from several pre-defined filters and/or any previous search in the session (stored in a history list). The combination of conventional search/match and Boolean searches can be very powerful, as illustrated in the next section.

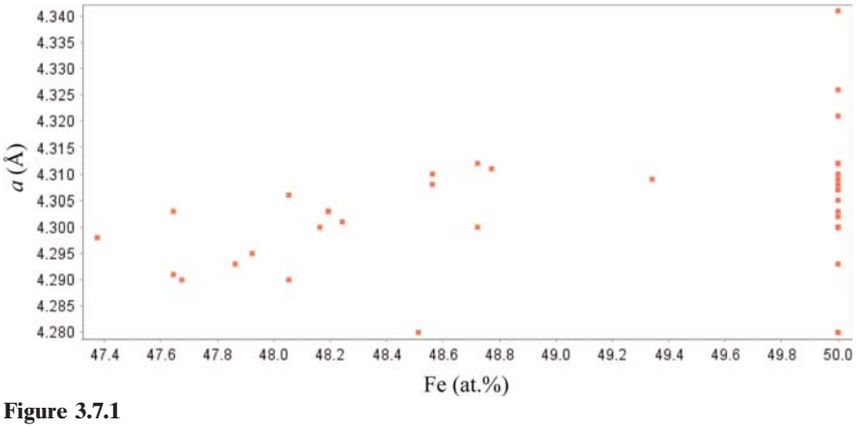

Figure 3.7.1
A plot generated by the Results/Graph Fields function in the Powder Diffraction File. The search was for entries containing only Fe and O and with space group No. 225 (resulting in FeO entries) measured under ambient conditions. One outlier was removed from the hit list manually. The trend in the cubic *a* lattice parameter with Fe content is apparent, as well as the large number of apparently stoichiometric FeO entries, some of which may not be correctly characterized.

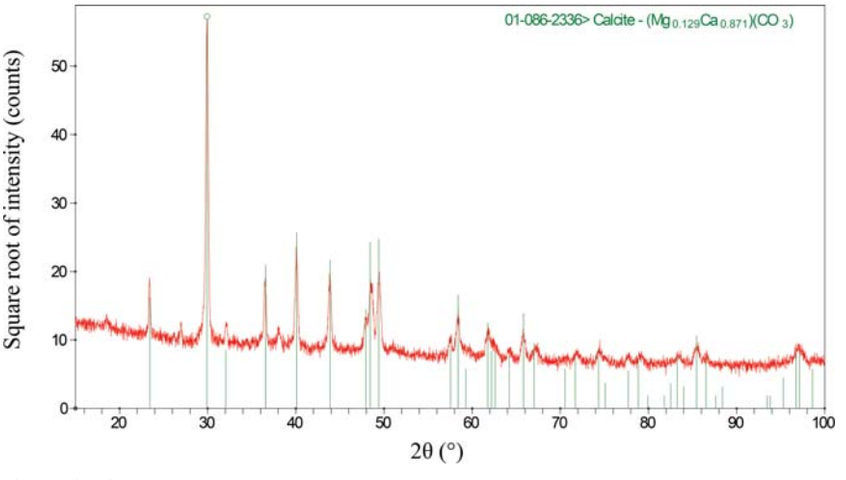

Figure 3.7.2
The result of applying a commercial search/match program (*Jade* 9.5; Materials Data, 2012) to the powder pattern of a water-still scale. Weak peaks not accounted for by the major magnesian calcite phase are apparent and additional tools in the Powder Diffraction File were needed to identify the additional phases.

3.7.2.4. *Boolean logic in phase identification*

Most phase identifications are carried out using the peak-based or full-pattern algorithms supplied by the instrument vendor. These often work well for major phases and can be customized to improve their success in identifying minor/trace phases. The native capabilities of the PDF (not all of which are accessible through some vendors' software) can be very powerful in identifying those extra peaks that result from a Rietveld difference plot (or any difference plot from pattern-fitting software) using the major phases. Below we use examples to illustrate several strategies.

3.7.2.4.1. *Water-still deposit*

A water still in my home eventually generates scale, much of which flakes off the walls, permitting easy analysis in the powder diffractometer. Any commercial search/match program will easily identify magnesian calcite (Fig. 3.7.2; files kadu1389.gsas, kadu1389.raw and iitd26_0510.prm, available in the supporting information). There are, however, three additional weak peaks at d/I = 4.788/38, 3.3089/51 and 2.3697/56. In Naperville, Illinois, the tap water comes from Lake Michigan. The bedrock underlying the Chicago region is the Racine Dolomite. Given the identity of the major phase in the scale and the source of the water, it seems likely that any minor phases will be mineral-related and contain some combination of the elements Ca, Mg, C, O and H (to include the possibility of hydrates and hydroxides). Accordingly, a search of mineral-related entries containing 'just' the elements Ca, Mg, C, O and H was performed and used as a filter in a Hanawalt search using these three peaks. This limits the search universe to 692 of the 328 660 entries in the PDF-4+ in 2012. The seven highest goodness-of-match entries in the hit list were brucite, $Mg(OH)_2$. This phase was added to the Rietveld refinement. Analysis of the difference plot indicated an unaccounted-for peak at a *d*-spacing of 3.3089 Å. A search for mineral-related entries with the same chemistry and having one of their three strongest peaks in the range 3.309 (30) Å yielded the vaterite polymorph of $CaCO_3$ as the hit with the highest goodness of match. This phase was added to the Rietveld refinement. The final quantitative phase analysis was: 94.7 (1) wt% $Ca_{0.84}Mg_{0.16}(CO_3)$, 5.2 (4) wt% $Mg(OH)_2$ and 0.2 (1) wt% vaterite.

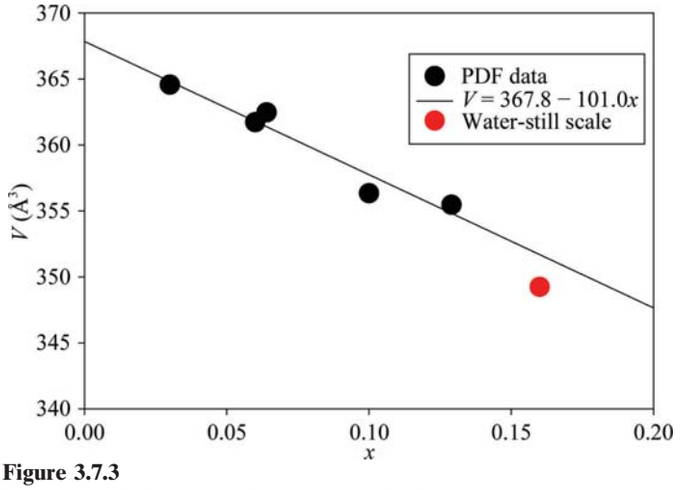

Figure 3.7.3
Variation of the unit-cell volume with the magnesium content in magnesian calcites in the Powder Diffraction File.

The composition of the major phase was refined, constraining the sum of the Ca and Mg site occupancies to equal 1.0. To understand how this fitted with previous magnesian calcites, a search for compounds containing only Ca, Mg, C and O, ambient conditions and space group No. 167 was carried out. Some manual editing of the hit list was required. Adjusting the preferences to include the display of composition in at.% and the unit-cell volume made it convenient to plot the variation in unit-cell volume as a function of Mg content x in $Ca_{1-x}Mg_x(CO_3)$ (Fig. 3.7.3). This magnesian calcite in the water-still scale has a higher Mg concentration than most, but falls close to the trend line. The flexibility and content of the Powder Diffraction File makes such data mining relatively straightforward.

3.7.2.4.2. *Vanadium phosphate butane-oxidation catalyst*

Vanadyl pyrophosphate [$(VO)_2P_2O_7$] catalysts are used commercially for the selective oxidation of butane to maleic anhydride. Modern third-generation search/match programs [using the background-subtracted, $K\alpha_2$-stripped data (files goed80.gsas, GOED80.raw and d8v3.prm); Fig. 3.7.4] had no trouble in identifying the desired major phase $(VO)_2P_2O_7$, but had difficulty with the minor phases that were clearly present. Unless the display of duplicate entries is turned off, most programs will yield several duplicate hits at the top of the list. Both 00-050-0380 and 04-009-2740 are Star quality, but only the Linus Pauling File (LPF) entry 04-009-2740 contains atom coordinates for a Rietveld refinement. Entry 01-070-8726 has the lower-quality B mark.

The native capabilities of the PDF proved helpful in identifying the minor phases. The lowest-angle peak not accounted for by the major phase is at a d-spacing of 7.2107 Å. A search for phases containing just the elements V, P, O and H (known from the synthesis procedure) and having one of their three strongest peaks in the range 7.21 ± 0.05 Å (an estimated range) yielded only the single hit 00-047-0967: $H_4V_3P_3O_{16.5}(H_2O)_2$. This is a low-precision (O quality mark) pattern from a US Patent (Harju & Pasek, 1983), and the pattern contains only four lines. The comments in the PDF entry indicate that this hydrated phase was formed by exposing a catalyst to ambient conditions, so it seems chemically reasonable but poorly defined.

To see whether this phase had been better characterized by a crystal structure, the four peaks were entered into *SIeve+* and a Hanawalt search using a wider than default tolerance of 0.3° on the peak positions and the 'just' chemistry filter V, P, O and H was carried out. As expected, PDF entry 00-047-0967 was at the top of the hit list, but close to the top was entry 04-017-1008 (Shpeizer *et al.*, 2001): $[H_{0.6}(VO)_3(PO_4)_3(H_2O)_3](H_2O)_4$. The article by Shpeizer *et al.* (2001) indicates that this phase was formed from an anhydrous precursor by exposing it to ambient conditions. The single-crystal structure was obtained at 173 K. The similarity of the two PDF entries (Fig. 3.7.5) and the difference in data-collection temperatures makes it clear that these correspond to the same phase, and that the structure of $[H_{0.6}(VO)_3(PO_4)_3(H_2O)_3](H_2O)_4$ could be used in a Rietveld refinement.

There were still unaccounted-for peaks at 3.5823 and 3.0760 Å. Under the assumption that these came from a single phase, two separate searches for phases containing just V, P, O and H and with one of their three strongest lines in the ranges 3.58 ± 0.03 and 3.08 ± 0.03 Å were carried out and then combined (using the History option) with a Boolean 'and' operation. All five of the entries on the hit list corresponded to α-$VOPO_4$. This yellow V^{5+} compound was consistent with the altered colour of the V^{4+}-based catalyst, and is a common impurity.

Close examination of the Rietveld difference plot from a refinement including these three phases indicated that there was a weak shoulder at a d-spacing of 3.985 Å. A search for phases containing just V, P, O and H and having a strong peak near this d-spacing yielded β-$(VO)(PO_3)_2$, another common catalyst impurity (Fig. 3.7.6). Including this compound as a fourth phase yielded a satisfactory Rietveld refinement and a quantitative analysis of 84.8 (1) wt% $(VO)_2P_2O_7$, 5.9 (1) wt% $[H_{0.6}(VO)_3(PO_4)_3(H_2O)_3](H_2O)_4$, 5.6 (1) wt% α-$VOPO_4$ and 3.7 (1) wt% β-$VO(PO_3)_2$.

3.7.2.4.3. *Valve deposit from a piston aviation engine*

Applying a commercial search/match program to the diffraction pattern of a deposit from a valve in a gasoline-powered aircraft engine easily identified quartz and corundum. The specimen was scraped from the valve seat and micronized. The corundum represents abrasion from the elements of the micronizing mill, as it was not present in the pattern of the as-scraped sample. Metal particles were visibly present in the deposit, so one could reasonably guess the presence of both ferrite and austenite (Fig. 3.7.7; files maso04.gsas, maso04.rd and padv.prm). A Rietveld refinement using these four phases was carried out.

Six peaks picked from the difference plot were entered into *SIeve+* and a Hanawalt search was carried out. No chemically reasonable simple compounds were near the top of the hit list, so extra information was sought. An XPS analysis indicated the presence of Pb, Br, Fe, P, O and C (and H assumed). Aviation gasoline is still leaded, and ethylene dibromide is sometimes added as a lead scavenger. The result of a 'just' chemistry search using these seven elements (6543/328 660 entries) was applied as a filter to the Hanawalt search. Near the top of the hit list was $PbBr_2$. Although apparently surprising, this phase is reasonable given our chemical knowledge. Lead bromide was added to the Rietveld refinement. Further analysis of the difference pattern using the same techniques indicated the presence of cohenite, Fe_3C, from the steel, and $Fe_3Fe_4(PO_4)_6$, the reaction product of the steel with a phosphate fuel additive. The final Rietveld refinement yielded a quantitative analysis of 26.5 (4) wt% austenite (γ-Fe, stainless steel), 47.9 (4) wt% ferrite (α-Fe, carbon steel), 17.7 (4) wt% quartz (sand/dirt), 2.9 (2) wt% $PbBr_2$, 2.6 (2) wt% $Fe_3Fe_4(PO_4)_6$ and 2.2 (2) wt% cohenite (Fig. 3.7.8).